

USE OF KRAMERS-KROING RELATIONSHIP FOR DIELECTRIC DIAGNOSIS

B.Hemalatha¹ Y.P.Singh² V G Rau²

¹Indian Institute of Technology Kharagpur India

²Retired Professor of Indian Institute of Technology Kharagpur India

*Email: <hema@adm.iitkgp.ernet.in>

Abstract: For a linear dielectric, the real and imaginary parts of the response are related through Kramers-Kroing relationship. This paper describes a numerical method for obtaining the Kramers-Kroing transform. The method has been applied to data measured experimentally in the laboratory on Epoxy Bonded Mica Tape, Electrical grade Capacitor paper and the insulation system of a 6.6kV rotating machine. The numerical method has been successfully used to check the consistency of the dielectric response data and isolate the *dc* conduction component at low frequencies.

1 INTRODUCTION

The real and imaginary parts of the dielectric response of a linear dielectric related to each other through the Kramers-Kroing relationship because they are derived from same exciting function [1,2]. These relationships are derived from the Hilbert's integral transforms. The relationships can thus be used for obtaining the data pertaining to the real part of the ideal dielectric response when only the imaginary part is available or vice versa. The case when the response data of a linear dielectric are not Kramers-Kroing compatible, when a strong *dc* conduction component is present in addition to the dipolar processes. This kind of response is found in many dipolar systems, especially at low frequencies and high temperatures. The presence of a *dc* conduction component is characterised by a sharp increase in the imaginary component, while the real part remains constant.

If ε' and ε'' are the real and imaginary parts of complex permittivity, then at a particular radian frequency ω_0 the Kramers-Kroing relationships can be expressed as:

$$H(\varepsilon''(\omega_0)) = \varepsilon'(\omega_0) - \varepsilon_\infty = \frac{2}{\pi} \int_0^\infty \frac{\omega \varepsilon''(\omega)}{\omega^2 - \omega_0^2} d\omega \quad ..(1)$$

$$H(\varepsilon'(\omega_0)) = \varepsilon''(\omega_0) = -\frac{2}{\pi} \omega_0 \int_0^\infty \frac{\varepsilon'(\omega)}{\omega^2 - \omega_0^2} d\omega \quad ..(2)$$

where $H(\varepsilon''(\omega_0))$ and $H(\varepsilon'(\omega_0))$ are the Hilbert's transforms of ε'' and ε' respectively. In the above equations the principal value of the integral is considered, excluding the point of singularity. This means that if the values of the real part of the permittivity over a wide range of

frequencies is known, then it is possible to obtain the imaginary part over the same range and vice versa. In practice, the limits of the integral in Equations (1) and (2) are limited to a finite range of measured frequencies. An important consequence of the integrals is their evaluation for zero frequency [2].

$$\begin{aligned} \varepsilon_s &= \varepsilon'(0) = \varepsilon_\infty + \frac{2}{\pi} \int_0^\infty \frac{\varepsilon''(\omega)}{\omega} d\omega \\ &= \varepsilon_\infty + \frac{2}{\pi} \int_0^\infty \varepsilon''(\omega) d(\ln \omega) \quad \dots(3) \end{aligned}$$

ε_s is the value of the permittivity at zero frequency and ε_∞ the value at very high frequencies. This relates the polarization increment for a given polarisation mechanism to the loss curve plotted against the logarithm of the given frequency. This immediately shows that a mechanism leading to stronger polarisation invariably gives rise to higher losses.

2 EVALUATION OF THE INTEGRAL

The principal value of the integral is evaluated by excluding a small region of radius r around the singular point $\omega = \omega_0$, where the integral just begins to diverge and the boundaries are approached equally fast from both sides. From equations (1) and (2), it is evident that the real or imaginary part of the permittivity at any frequency, ω_0 , depends on the value of the other at all frequencies with the significance of the value decreasing as $\omega^2 - \omega_0^2$ becomes larger. When $\omega \leq \omega_0$, the function inside the integral and the integral itself tends to a constant value, while for $\omega \geq \omega_0$, the integral almost tends to zero. This fact is exploited while performing a numerical transform

over a finite range of frequencies. Since the real part of the permittivity is a continuous function of the frequency and remains positive over the range of frequencies considered, the integrand is negative, below the frequency of interest ω_0 , (which incidentally becomes the point of singularity) and positive above ω_0 . The integrand thus has a sign change around the singularity. The integral is split up into two halves, one corresponding to the region below ω_0 and the other above ω_0 . A region of radius r around ω_0 where the integral just begins to diverge is excluded and this numerical integration is carried out by using Newton-Cotes method [3]. The region $\omega_0 - r$ and $\omega_0 + r$ is evaluated by integrating equation (1) by parts since the derivatives of $\varepsilon''(\omega)$ in this region are bounded. Up to 3 significant terms are considered in the repeated integration. The principal value of the integral is thus evaluated as

$$\varepsilon'(\omega_0) - \varepsilon_\infty = \frac{2}{\pi} \left[\int_{\omega_1}^{\omega_0-r} I d\omega + \int_{\omega_0+r}^{\omega_2} I d\omega + \int_{\omega_0+r}^{\omega_2} I d\omega \right] \dots(4)$$

where

$$I = \frac{\omega \varepsilon''(\omega)}{\omega^2 - \omega_0^2}$$

ω_1 and ω_2 are the lowest and highest available frequencies respectively. The value of r is chosen as the point where the function just begins to diverge. Figure 1 depicts the variation of the integrand with ω . Equal halves are considered on either side of ω_0 . The accuracy of the results will be determined by the highest and lowest frequency up to which the data is available and the number of terms used in the repeated integration by parts. In order to make fullest possible use of the finite range of measured frequencies, the measured results are extrapolated by one decade on either end. A similar procedure is adopted for obtaining the Kramers-Kroing transform of the real part to obtain the imaginary part of the permittivity.

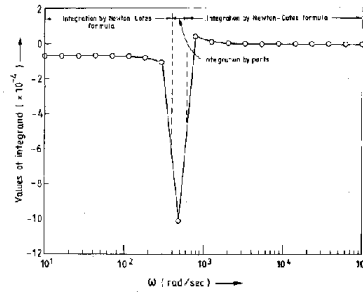


Figure 1: Variation of Integrand (equation (4))

2.1 Example: Ideal Case

Consider the Havriliak-Negami model:

$$\varepsilon^* = 2 + \frac{15}{\left(1 + (100j\omega)^{0.8}\right)^{0.8}} \dots(5)$$

The real part of the data is computed with 5 points per decade in the range $\omega = 10$ rad/sec to $\omega = 100000$ rad/sec. Using the Kramers-Kroing transform the imaginary part is derived. The data is first of all extrapolated by one decade on either side of the spectrum, i.e., upto 1rad/sec on the low frequency side and upto 1000000 rad/sec on the high frequency side. Consider a point $\omega_0 = 500$ rad/sec. A small region of radius r in the neighbourhood in the region of singularity is cut out such that $\frac{\omega_0}{\omega_0 - r} = \frac{\omega_0 + r}{\omega_0}$ that is the points $\omega_0 + r$ and $\omega_0 - r$ are symmetrically located on a logarithmic scale around ω_0 . Taking this ratio as 0.8, for a frequency of 500 rad/sec., the upper limit of the first integral of equation (4) is thus 400 rad/sec and the lower limit of the third integral is 425 rad/sec. The region between 1 rad/sec and 400 rad/sec and that between 625 rad/sec to 1000000 is integrated by using the Newton cotes formula. The region between 400 to 625 rad/sec which contains the point of singularity is integrated by parts considering the first three terms of the repeated integration. The integral is thus defined as

$$\varepsilon''(500) = \frac{2}{\pi} 500 \left[\int_1^{400} I d\omega + \int_{400}^{625} I d\omega + \int_{625}^{1000000} I d\omega \right] \dots(6)$$

where $I = \frac{\varepsilon'(500)}{\omega^2 - 500^2}$, this works out to

be

$$\varepsilon''(500) = \frac{2}{\pi} 500(-0.0366) + 0.1057 + \frac{2}{\pi} 500(0.0393) = 0.97$$

The value of the integral at 500 Hz is thus 0.97. In

this case ϵ'' is available at 20 discrete points between $\omega = 10$ to 1000000 rad/sec. While evaluating the integral values of ϵ' at points other than the measured frequencies are required, for this a cubic spline interpolation method is used to generate data between the measured values.. Table 1 lists the values of ϵ'' obtained by using the Kramers-Kroing transform. The other transform for obtaining real part of the data using the imaginary part is carried out in a similar way.

Table-1 Kramers-Kroing Transforms of the Ideal System

ω rad/sec.	ϵ''	$H(\epsilon'(\omega))$	$\epsilon' - \epsilon_{\infty}^*$	$H(\epsilon''(\omega))$
10	0.0453	0.0156	14.98	14.49
50	0.1633	0.1324	14.95	14.35
100	0.2826	0.2283	14.90	14.25
500	0.9824	0.9742	14.59	13.92
1000	1.6314	1.6010	14.22	13.89
5000	4.146	4.0616	11.45	11.05
10000	4.9173	4.7601	8.95	8.09
50000	3.5696	3.0464	3.36	2.86
100000	2.5515	2.2004	2.06	1.72

The above table indicates that the accuracy of the estimates come down drastically at the edge of the frequency spectrum. The estimates are best when adequate number of data points are available on either side of the frequency of interest.

2.2 Experimental Data

A) Epoxy Mica Tape: The complex permittivity of 0.05mm thick Epoxy bonded Mica Tape at room temperature conditions was measured over a frequency range of 10 Hz to 10 kHz with 3 points per decade using a Frequency Response Analyser in conjunction with an Electrochemical Interface [4,5]. The response characteristics so measured are shown in Figures 2a and 2b respectively. The Kramers-Kroing compatibility of this data is checked by the extrapolating the data by one decade on either side of the spectrum to improve the accuracy of the transform on edges of the frequency spectrum. The Kramers-Kroing transforms for the real and imaginary parts are shown in Table 2 and they show a reasonably good agreement with the experimentally measured values in the region 10 Hz-10 kHz.

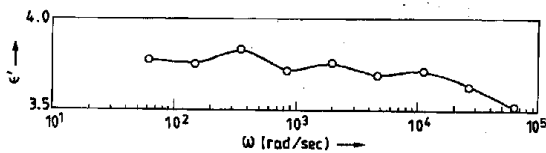


Figure 2a: Variation of ϵ' with Radian Frequency for Epoxy Bonded Mica

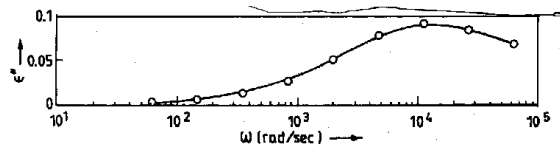


Figure 2b: Variation of ϵ'' with Radian Frequency for Epoxy Bonded Mica Tape

Table-2 Kramers-Kroing Compatibility for Epoxy Mica Tape

ω rad/sec.	ϵ''^*	$H(\epsilon'(\omega))$	$\epsilon' - \epsilon_{\infty}^*$	$H(\epsilon''(\omega))$
1	0.0003	0.0015	14.98	14.79
10	0.0031	0.0021	14.95	14.69
100	0.0224	0.0189	14.90	14.58
1000	0.0866	0.0845	14.59	14.32
10000	0.0706	0.0631	14.22	13.99
100000	0.0249	0.0322	11.45	10.65

* Experimentally measured

B) Capacitor Paper: The permittivity characteristics of 0.04mm thick capacitor paper are measured at room temperature in the region 25 Hz to 100 kHz with 3 points per decade are shown in Figures 3(a) and Figure 3(b) respectively. From the graphs, it is evident that the slope at the low frequency end is negative and increases with respect to frequency, then begins to decrease and finally tends to a constant value. The negative slope indicates the presence of a dc component in the dielectric response. It is important to observe that this crosses the zero point twice. The first point where it crosses the zero corresponds to the point where the dc component just begins to dominate and the second point corresponds to the loss peak frequency. Comparing the variation of the real part of the permittivity and the imaginary part of the permittivity with frequency, it is seen that while the loss component shows a sharp increase with decrease in frequency, the real part is more or less constant. This confirms the presence of a dc conduction component.

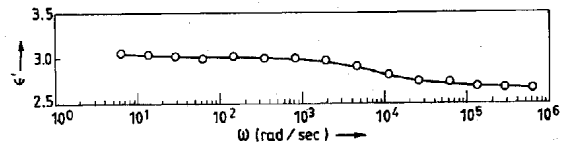


Figure 3a: Variation of ϵ' with Radian Frequency for Capacitor Paper

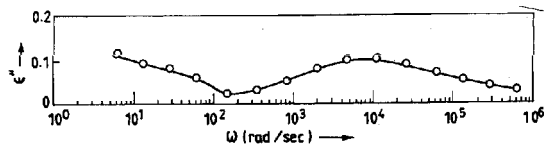


Figure 3b: Variation of ϵ'' with Radian Frequency for Capacitor Paper

The Kramers- Kroing transform of the real part of the permittivity is obtained to give the imaginary part. This is subtracted from the measured ϵ'' to give the estimated conductive part. Since the estimates of the actual dielectric component are lower than that actually expected, the actual conductive component will be little higher. A graph of the variation of the conductive part with frequency is shown in Figure 3c. The conductive part shows a drastic decrease with increase in frequency and becomes negligible beyond 150 Hz.

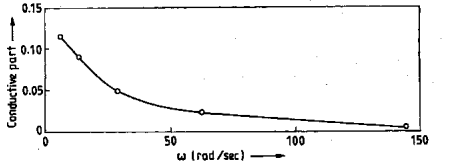


Figure 3c: Variation of dc conductive portion with Radian Frequency for Capacitor Paper

C) Insulation System of a 6.6kV rotating machine: In the case of a practical insulation system, the geometry of the dielectric is complex it is difficult to arrive at the complex permittivity. The dielectric loss tangent $\tan \delta$ which is independent of the geometry is considered. The loss tangent is the ratio of C''/C' , where C'' is the imaginary part of

the impedance and C' the real part. The impedance spectra are also measured using the Frequency Response Analyser [4,5]. Such spectra can be of vital use in diagnosing the condition of the insulation. The complex impedance characteristics for a rotating machine coil using epoxy bonded mica resin as the main wall insulation with a geometry specified in Figure 4 is measured at room temperature between 1Hz to 100 KHz with 5 points/decade. The variation of the real and imaginary part of the response is shown in Figure 5. The presence of a dc conduction component is evident. Using the same technique outlined above the conductive portion is obtained by using the Kramers-Kroing transform.

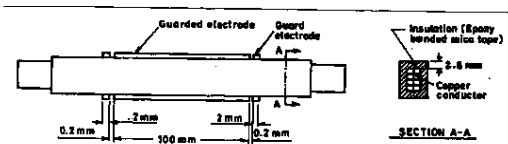


Figure 4: Cross section of main insulation of a 6.6 kV rotating machine coil

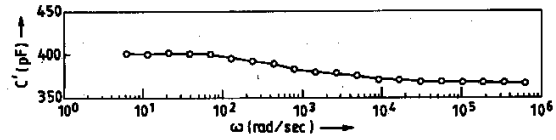


Figure 5a: Variation of ϵ' with Radian Frequency for Rotating Machine Coil Insulation

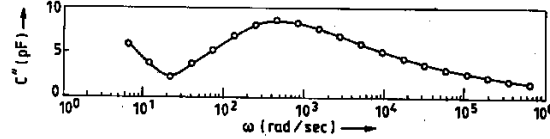


Figure 5b: Variation of ϵ'' with Radian Frequency for Rotating Machine Coil Insulation

In this case too, the conductive part is high at low frequencies and tapers off as the frequency increases.

3 CONCLUSION

This paper has proposed a numerical method for evaluating the Kramers-Kroing integral. The method has been successfully applied in extracting the real part of the response spectrum when the imaginary part is available and vice versa to the experimentally measured data in the laboratory. The accuracy of the estimates are best around the central region of the measured frequency spectrum. Whenever, a strong dc conduction component is present, using the Kramers-Kroing transform it is possible to separate out the conductive portion from the overall portion of the dielectric response. The degree and deviation from the Kramers-Kroing compatibility can serve as a useful aid in dielectric diagnosis.

4 REFERENCES

- [1] 2. H. A. Kramers, *Aiii. Cong. Intern. Fisici*, Como, 2, 1927, p.545
- [2] A.K.Jonscher, *Dielectric Relaxation in Solids*, Chelsea Press 1983.
- [3] Hilderbrand.F.B., *Introduction to Numerical Analysis*, Tata McGraw Hill ,New Delhi 1974.
- [4] J.Pugh, *Dielectric Measurements using Frequency Response Analyzers* , IEE Pub no. 279, pp 247-250, 1984.
- [5] B.Hemalatha, *Frequency Domain Modelling of Linear Dielectric Systems and Techniques for Identification of Model Parameters*, Ph.D thesis, IIT Kharagpur, 1997.